JOURNAL OF GEOPHYSICAL RESEARCH: ATMOSPHERES, VOL. 118, 6281–6289, doi:10.1002/jgrd.50506, 2013

Reconciliation of modeled climate responses to spectral solar forcing

Guoyong Wen,[1,2] Robert F. Cahalan,[1] Joanna D. Haigh,[3] Peter Pilewskie,[4] Lazaros Oreopoulos,[1] and Jerald W. Harder[4]

Received 12 November 2012; revised 15 May 2013; accepted 16 May 2013; published 26 June 2013.

[1] The SIM (Spectral Irradiance Monitor) on SORCE (Solar Radiation and Climate Experiment) provides more spectrally complete daily SSI (spectral solar irradiance) measurements than ever before, allowing us to explore chemical and physical processes in the Earth's ocean and atmosphere system. However, the newly observed SSI instigated controversies in the Sun-climate community on whether the SIM-observed trends are true solar variations and on whether climate responses are in phase or out of phase with solar forcing. In this study, we focus on resolving two apparently contradictory results published on possible temperature responses to SIM-derived solar forcing. When applying extreme scenarios of SIM-based spectral solar forcing in a radiative-convective model (RCM), we find that some apparently contradictory results can be explained by the different methods used to apply the SIM SSI data. It is clear that accurate SSI data are essential for accurate climate simulations and that climate modelers need to take care how they apply these data.

Citation: Wen, G., R. F. Cahalan, J. D. Haigh, P. Pilewskie, L. Oreopoulos, and J. W. Harder (2013), Reconciliation of modeled climate responses to spectral solar forcing, *J. Geophys. Res. Atmos.*, *118*, 6281–6289, doi:10.1002/jgrd.50506.

1. Introduction

[2] Satellite observations over the past three decades reveal a ~0.1% increase in TSI (total solar irradiance) from solar minimum to solar maximum in the 11 year solar activity. The recent TIM (Total Irradiance Monitor) instrument on NASA's SORCE (Solar Radiation and Climate Experiment) satellite has provided the most accurate TSI values of 1360.8 ± 0.5 W/m^2 during the 2008 solar minimum as compared to 1365.4 ± 1.3 W/m^2 established in the 1990s [*Kopp and Lean*, 2011]. Thus, both the relative variation from the solar minimum to the maximum in the 11 year solar activity and the absolute value of TSI and associated uncertainties in the solar minimum of solar cycle 23 are well established. The question of whether there is a trend from one solar minimum to another awaits to be determined in future solar missions such as the Total and Spectral Irradiance Sensor.

[3] Consistent with global observations from satellites [*Loeb et al*., 2009], a recent study has stated that "Earth is absorbing more energy from the Sun than it is radiating to space as heat, even during the recent solar minimum" [*Hansen et al*., 2011]. Among other parameters, accurate and continuous observation of the TSI, the input energy to the Earth system, is required to monitor the energy imbalance from space and to understand the causes of changes in the Earth's radiation budget over time. Yet the TSI alone is not sufficient for understanding the physical processes in the Earth's ocean and atmosphere system. Using a simple climate model, *Cahalan et al*. [2010] showed that even for the same TSI variation, atmospheric and ocean temperatures have significantly different responses depending on the details of SSI (spectral solar irradiance) variations. Thus, accurate observations of both TSI and SSI are required for Sun-climate studies.

[4] The variation of SSI in the 11 year solar activity cycle and its absolute accuracy has not yet been firmly established. In the 1980s and 1990s, several missions were carried out to observe the solar ultraviolet spectrum (see *DeLand and Cebula* [2012]for review). *DeLand and Cebula* [2008] were able to provide a composite observation from different satellite platforms. However, as stated by *Ball et al*. [2011], "this only accounts for absolute differences between different instruments and does not take into account instrumental problems and trends and so requires further adjustments before being truly useful for climate studies." Before the launch of SORCE in 2003, there was no continuous observation of SSI variability, in both wavelength and temporal domains, over the visible and infrared portions of the spectrum longward of 400 nm that accounts for about 90% of the total solar output.

[5] The SIM (Spectral Irradiance Monitor) instrument on the SORCE satellite makes, for the first time, daily observations of SSI from 200 to 2423 nm, covering almost the entire energy-bearing solar spectrum (i.e., total energy, not energy per photon). *Harder et al*. [2009] found that from 2004 to

[1]NASA Goddard Space Flight Center, Greenbelt, Maryland, USA.
[2]Goddard Earth Sciences Technology and Research, Morgan State University, Baltimore, Maryland, USA.
[3]Blackett Laboratory, Imperial College London, London, UK.
[4]Laboratory for Atmospheric and Space Physics, University of Colorado Boulder, Boulder, Colorado, USA.

Corresponding author: G. Wen, NASA Goddard Space Flight Center Code 613, Greenbelt, MD 20771, USA. (Guoyong.Wen-1@nasa.gov)

2169-897X/13/10.1002/jgrd.50506

2007, during the descending phase of solar cycle 23, the SIM VIS (visible) and NIR (near-infrared) spectral irradiance had an increasing trend which opposed a decreasing trend in the UV (ultraviolet). They also found that the variation in UV spectral irradiance was about 4–6 times larger than that reported by the NRL (Naval Research Laboratory) empirical model [*Lean*, 2000]. Motivated by this discovery, several research efforts have suggested that the temperature and ozone response to SIM-observed spectral solar forcing would be quite different from the responses to the estimated spectral solar forcing based on the NRL model [e.g., *Cahalan et al*., 2010; *Haigh et al*., 2010; *Merkel et al*., 2011; *Ineson et al*., 2011; *Swartz et al*., 2012].

[6] The SIM observations and subsequent atmospheric modeling studies have introduced some controversy to the Sun-climate community. One important issue is whether the SSI variation observed by SIM in the descending phase of solar cycle 23 is real. Some studies show disagreement between observed SIM SSI and modeled SSI [e.g., *Ball et al*., 2011; *Lean and DeLand*, 2012]. From a comparison of the SIM and NRL SSI, *Lean and DeLand* [2012] concluded that "the SIM's radically different solar variability characterization is a consequence of undetected instrument sensitivity drift." Another study, however, has shown agreement between the SIM observations with another modeled SSI: *Fontenla et al*. [2011] found that the Solar Radiation Physics Model does capture the antisolar cycle trends reported by SIM and, furthermore, is in agreement with the findings of *Preminger et al*. [2011] from San Fernando Observatory.

[7] Another controversial issue is whether the surface temperature responses to SIM spectral solar forcing are in phase or out of phase with solar activity. Using SIM SSI as input to a 2-D climate model, *Haigh et al*. [2010] found that solar radiative forcing is out of phase with solar activity. Without computing temperature responses, Haigh et al. made a tentative conclusion that their findings "raise the possibility that the effects of solar variability on temperature throughout the atmosphere may be contrary to current expectations." In an independent study, however, using an 11 year solar cycle based on SIM as input to a one-dimensional (1-D) radiative-convective model (RCM), *Cahalan et al*. [2010] found in-phase surface-tropospheric temperature responses with solar activity and stratospheric responses similar to Halogen Occultation Experiment observations.

[8] The present study is motivated by these issues. We focus particularly on understanding and reconciling the apparently contradictory results of Haigh et al. and Cahalan et al. The background information and method are presented in section 2, section 3 presents the results of the study, followed by a summary and discussion of the results in the final section.

2. Background and Approach

[9] To better understand the difference between the study by *Haigh et al*. [2010] (hereinafter H2010) and that by *Cahalan et al*. [2010] (hereinafter C2010), we briefly describe their approaches. We then design and perform experiments to demonstrate why their conclusions are different.

2.1. Review of the Two Studies

[10] Both H2010 and C2010 explored the climate response to two formulations of the spectral solar forcing, one is based on the NRL empirical model by *Lean* [2000], and the other is based on SIM observations [*Harder et al*., 2009]. Here we focus on the SIM-based spectral solar forcing experiments.

[11] Although both H2010 and C2010 studied climatic responses, there are several notable differences between the two studies. First, the models and foci of the two studies are different. H2010 used a 2-D radiative-photochemical model to compute the equilibrium states for April 2004 and November 2007 focusing on the responses in stratospheric ozone. C2010 used a 1-D ocean-atmosphere coupled RCM to compute time-dependent temperature responses to SIM-based 11 year solar forcing.

[12] Second, the input solar forcings are different in the two studies, even though both used the SIM data. The *Harwood and Pyle* [1975] model used by Haigh et al. interpolates the solar spectrum onto the 171 wave bands in the range of 116–730 nm for computing photochemical processes in the middle atmosphere. Variations of spectral irradiance above 1600 nm are neglected.

[13] C2010 used the full SIM spectral wavelength from 200 to 2423 nm with the coarse spectral resolution in *Harder et al*. [2009, Figure 3]. C2010 also introduced irradiance in addition to that derived from the SIM data such that the spectrally integrated energy equals exactly that of the TIM TSI. Such an irradiance constraint is not considered by H2010.

[14] The two studies have very different results for radiative forcing. H2010 did not compute the surface temperature response, but they estimated downward irradiances at the tropopause and suggested an out-of-phase surface temperature response to solar activity. C2010 computed temperature profiles and showed quantitatively that surface temperature has a small but in-phase response to SIM-based sinusoidal 11 year spectral forcing.

[15] To avoid any issues related to the use of different atmospheric models, we apply spectral forcings similar to those used by H2010 and C2010 in the same RCM to compute the equilibrium state for April 2004 and November 2007. We first briefly describe the RCM and the spectral irradiance inputs used and then present results in the next section.

2.2. Radiative Convective Model

[16] The 1-D climate model in this study treats the atmosphere and ocean separately but couples them through energy exchange. A RCM is used for the atmosphere, as in many climate sensitivity studies [e.g., *Manabe and Wetherald*, 1967; *Lindzen et al*., 1982; *Arking*, 2005; *Liou and Ou*, 1983]. A 1-D heat diffusion model is applied to the ocean. The ocean-atmosphere coupling we adopt here is similar to that in Energy Balance Climate/Box Ocean Models [e.g., *Dickinson*, 1981; *Schlesinger et al*., 1985].

[17] Radiation models developed for climate research [*Chou and Suarez*, 2002; *Chou et al*., 2003] are used to compute radiative heating rates and associated temperature changes in the RCM. The solar radiation model computes the heating rate between 0.01 hPa and the surface with 5% accuracy. The thermal infrared radiation model computes fluxes and heating/cooling rates to within 1% accuracy compared to a high spectral resolution line-by-line calculation. The cooling rate can be computed accurately from the surface to the 0.01 hPa level. A convective adjustment scheme [*Manabe and Wetherald*, 1967] is applied to simulate the

Table 1. Cloud Properties Employed in the RCM

Cloud	Top Pressure (mb)	Amount (%)	Optical Thickness
High	267	19.4	2.2
Middle	560	19.	3.0
Low	820	28.	5.0

atmospheric heating due to convective processes. The RCM does not have interactive ozone chemistry.

[18] We apply the RCM to the tropics with a standard atmosphere O_3 profile and a constant CO_2 mixing ratio of 330 ppm throughout the atmosphere. Water vapor concentrations are computed interactively using the assumption of relative humidity as a fixed function of pressure [*Manabe and Wetherald*, 1967]; this is based on the observed vertical distribution of relative humidity and is a simple way to account for water vapor feedback. Using fixed relative humidity, *Manabe and Wetherald* [1967] found the sensitivity of surface temperature to CO_2 to be increased by a factor of ≈ 1.7 compared to that obtained with fixed water vapor concentrations (see review paper by *Held and Soden* [2000]).

[19] Three cloud layers (low, middle, and high) are inserted in the RCM. The cloud properties are taken from the cloud climatology reported by *Rossow and Schiffer* [1999] and are summarized in Table 1. The ocean albedo is assumed to be 0.07. A daytime length fraction of 0.5 and an average cosine solar zenith angle of 0.587 are used for tropical conditions. To compare the temperature difference between 2004 and 2007, we present simulations for equilibrium states. The SSI input and the experiment design are described in the next subsection.

2.3. Spectral Solar Forcing

[20] Before proceeding to the detailed analysis, we first present the spectral characteristics of the solar radiation model and the irradiances and variabilities in those bands.

[21] There are 11 broad spectral bands: seven in the UV (0.175–0.4 μm), one in the visible (0.4–0.7 μm), and three in the solar infrared (0.7–10 μm). We integrate the SIM spectral irradiance to obtain the 11 band irradiances. We also apply 10 day averaging to obtain two solar spectra, one each for April 2004 and November 2007.

[22] Figure 1, top shows the band irradiances in April 2004 and their absolute (Figure 1, middle) and relative (Figure 1, bottom) changes between April 2004 and November 2007 (2004 minus 2007), respectively. The sum of band irradiances in the entire SIM spectral range and associated changes as well as the TIM-observed TSI and associated variations are also presented in the same figure. All values are plotted on a log scale to emphasize the large range of variations. Note that band 11* (2.27–2.423 μm) covers only a portion of the model band 11 (2.27–10.0 μm) due to the upper

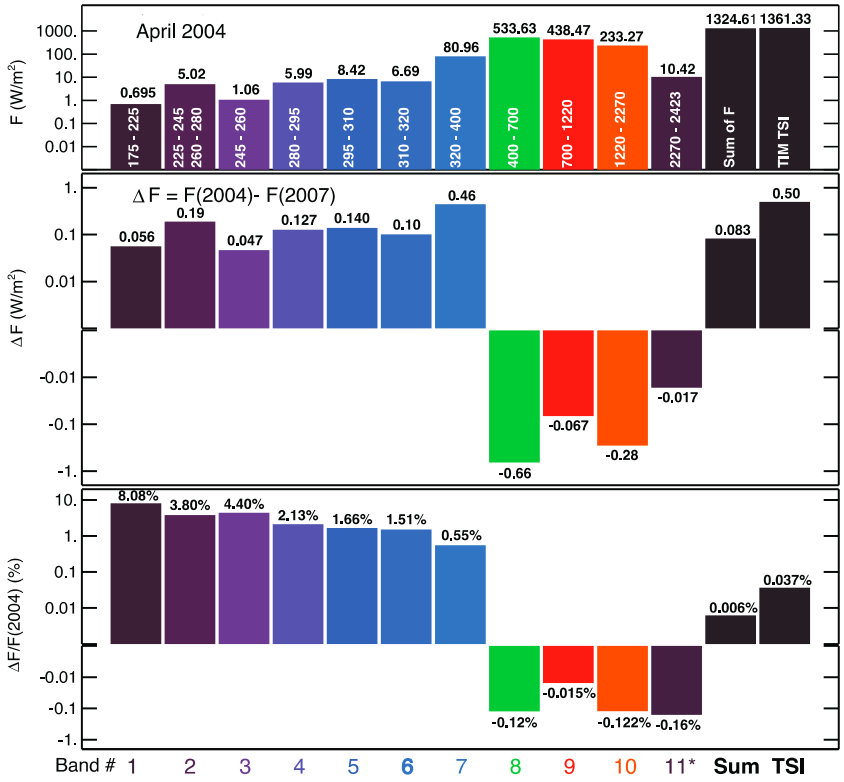

Figure 1. (top) SIM-observed irradiances in the 11 bands of the RCM's solar radiation model in April 2004 with the integrated SIM SSI and TIM TSI indicated. The wavelength ranges (in nanometers) of 11 bands are indicated in the color bars. (middle) The absolute changes (April 2004 minus November 2007) in solar irradiance for each solar band, integrated SIM SSI, and TIM TSI. (bottom) The relative changes in solar irradiance. Note that band 11* (2.27–2.423 μm) of the SIM SSI covers a portion of band 11 (2.27–10.0 μm) of the radiation model. SIM accounts for 97.3% of TSI, and the unobserved energy beyond the SIM wavelength is 36.72 W/m^2, about 2.7% of TSI.

limitation of the SIM spectral range. The main features of the spectral irradiance variations are summarized below.

[23] Figure 1 indicates that UV radiation has the largest relative change from 2004 to 2007. Within the UV spectrum, the percentage change increases with decreasing wavelength, from 0.55% in UV-A (320–400 nm) to 8% for the 175–225 nm band. The percentage changes in VIS and NIR are about 0.16% or less and out of phase with UV irradiance variation. Though the relative changes in UV-A, VIS, and IR spectra are small compared to changes in UV-C (175–280 nm) and UV-B (280–320 nm), the absolute changes are much larger than those in UV-C and UV-B. Thus, the variations in the UV-A, VIS, and NIR spectra are the most important components for direct climate forcing.

[24] The SIM SSI integrated irradiance from 200 to 2423 nm is 1324.61 W/m^2, accounting for 97.3% of the TIM-observed TSI of 1361.33 W/m^2 similar to *Harder et al*. [2009]; however, the change in integrated SIM SSI does not equal the change in TSI observed by TIM. The change in integrated SIM SSI from April 2004 to November 2007 is 0.08 W/m^2 or 16% of TIM-observed TSI variation of 0.5 W/m^2.

[25] This difference (0.08 W/m^2 versus 0.5 W/m^2) is unlikely to be due to unobserved irradiance variations beyond the SIM wavelength. This is because, to account for the missing energy ($\sim$36.72 W/m^2 in Figure 1), the change in infrared radiation would have to be 1.1% or 10 times as large as that in the visible and near-infrared region spectrally close to this region ($\sim$0.1% in Figure 1). Rather, it suggests that SIM cannot provide a sufficiently accurate measurement of TSI. This is consistent with the results of *Thuillier et al*. [2003]. In that study, SSI was integrated from 200 to 2400 nm using the Solar Spectrum (SOLSPEC) observations and the complement above 2400 nm computed from both the modeled spectrum of *Kurucz and Bell* [1995] and the spectrum of *Labs and Neckel* [1968] to yield TSI values of 1386.86 and 1387.29 W/m^2, respectively. Both derived TSI values are about 20 W/m^2 larger than the radiometric TSI of 1365.13 W/m^2 stated by *Crommelynck et al*. [1996]. The 20 W/m^2 discrepancy is about four times larger than the TSI bias error of $\sim$5 W/m^2 estimated from the current TSI value of 1360.8 ± 0.5 W/m^2 [*Kopp and Lean*, 2011]. *Thuillier et al*. [2003] pointed out that "a difference of 20 W/m^2 cannot be attributed to the UV domain, but more likely to the visible domain and IR domain, but to less extent" and "very likely the systematic uncertainty affecting the pyrometer calibration is the main source of the 1.4% difference found in this study." This inability of spectrometer observations to derive TSI is due to fundamental limitations of current technology for instrument calibration. As *Thuillier et al*. [2003] concluded: "The absolute accuracy, based on a detailed analysis of the sources of uncertainties, indicates a mean absolute uncertainty of 2 to 3%. This analysis shows that the largest sources of uncertainties are the pyrometer calibration, the weakness of the signal during calibration measurements at both ends of the spectral range and after filter changes during the spectral scanning." This is the reason that C2010 decided to apply a total irradiance constraint based on the independent TIM measurements of TSI.

[26] The increase of $\sim$0.1 W/m^2 (or $\sim$0.1%) in SIM irradiance between 2004 and 2007 in the range of 1630–2423 nm found by *Harder et al*. [2009] (their Figure 1g) was neglected by H2010. Its inclusion would tend to enhance their conclusion of an out-of-phase solar radiative forcing. Their neglect, however, of the total irradiance constraint might lead to errors in computing radiative forcing at the tropopause and, by implication, the surface temperature response.

[27] Similarly, the coarse resolution (same proportional change in UV) used by C2010 is not accurate, since percentage variability is not uniform across the UV spectrum, as shown in Figure 1 (bottom). In fact, the coarse resolution will lead to errors in distributing the energy change in the UV spectrum and to errors in computing temperature responses—even if the variation in TSI is correct. In the following section, we design experiments to investigate the approximations made and the differences found between the two studies.

3. Radiative Forcing and Temperature Response

[28] We design three spectral solar forcing scenarios for examining temperature responses. The first (SSF1) is similar to that in H2010: Only changes in SSI in the wavelength region of 200–1600 nm are considered, with SIM wavelength resolution used to determine the band irradiances, neglect of irradiance variations for wavelengths greater than 1600 nm, and no account taken of any constraint on the change in TSI.

[29] The second spectral solar forcing scenario (SSF2) is similar to that in C2010: The full SIM spectral range of 200–2423 nm is considered, but the variation in UV irradiance at 200–400 nm (of $\sim$1 W/m^2 from *Harder et al*. [2009], Figure 3) is distributed proportionately across all seven UV bands in our model. In order to ensure that the band summed TSI is equal to that from TIM measurements, the SIM unobserved energy (TIM-observed TSI minus integrated SIM SSI) is evenly distributed across the model's NIR bands for both April 2004 and November 2007. We assessed the sensitivity to inserting some of this difference into the visible band and found little difference in tropopause forcing and temperature response.

[30] The third spectral solar forcing (SSF3) uses the original full spectral resolution SIM data to derive the 11 band irradiances. The irradiance constraint is applied to the NIR bands.

[31] The changes in spectral band irradiance and shortwave irradiance are presented in Table 2. It is clear that input irradiance changes are very different for three forcing scenarios. In particular, the extra radiation introduced by the TSI constraint and applied to the NIR band (0.7–10 μm) means that the negative value given by the SIM data in the 0.7–1.6 μm region (for SSF1) becomes positive when SIM data in the 0.7–2.4 μm region are used (for SSF2 and SSF3) and that the total SW change increases from 0.23 to 0.50 W m^{-2}. The atmosphere is expected to show different responses to these scenarios. We present detailed analyses of vertical profiles of irradiance change only for SSF1 and SSF2 in sections 3.1 and 3.2 and show surface temperature responses for all three experiments in section 3.3.

3.1. Radiative Forcing Without Ozone Response

[32] For each given solar forcing input, we run the RCM until an equilibrium state is reached. We present the atmospheric profiles of irradiance difference (2004 minus 2007) for the different scenarios.

Table 2. The Input Irradiance Difference for UV-B-C, UV-A, VIS, and NIR and SW (April 2004 Minus November 2007) for Three Scenarios[a]

	UV-B-C (0.2–0.32 μm)	UV-A (0.32–0.4 μm)	VIS (0.4–0.7 μm)	NIR (0.7–10 μm)	SW (0.2–10 μm)
SSF1 (W m^{-2})	0.66	0.45	−0.65	−0.23	0.23
SSF2 (W m^{-2})	0.28	0.82	−0.65	0.04	0.50
SSF3 (W m^{-2})	0.66	0.45	−0.65	0.04	0.50

[a]For NIR (0.7–10 μm), SSF1 only accounts for SIM SSI variations in 0.7–1.6 μm, and SSF2 and SSF3 use SIM SSI in 0.7–2.4 μm and TSI constraint.

[33] We use the convention of downward positive and upward negative (i.e., downward flux ≥ 0, upward flux < 0, and net flux = downward flux + upward flux) throughout the remainder of the paper. Except for the different sign for upward flux, the change in net (down plus up) irradiance (solar plus longwave) at the tropopause is just the radiative forcing, the same as that used in other climate studies [e.g., *Ramaswamy et al*., 2001; *IPCC*, 2007]. With our convention, a positive downward irradiance difference means a larger irradiance value in 2004 than that in 2007, and a negative downward difference means a smaller irradiance value in 2004 than that in 2007; the opposite applies for upward irradiance differences.

[34] The vertical profiles of downward irradiance differences for UV, VIS, and NIR are presented in Figure 2. First, we examine the TOA (top-of-atmosphere) irradiance changes. It is clear that the input VIS irradiance differences (−0.19 W/m^2) are the same for both SSF1 and SSF2. However, the TOA irradiance differences in UV and NIR bands and total SW are very different for the two forcing scenarios. For SSF1, the irradiance changes are 0.19 W/m^2 (UV-B-C), 0.13 W/m^2 (UV-A), −0.07 W/m^2 (NIR), and 0.06 W/m^2 (SW), as compared to 0.08 W/m^2 (UV-B-C), 0.24 W/m^2 (UV-A), 0.01 W/m^2 (NIR), and 0.14 W/m^2 (SW) for SSF2.

[35] Both SSF1 and SSF2 have same changes in downward UV irradiances (UV-B-C plus UV-A). Since the UV irradiance exhibits a smaller percentage change at longer wavelengths than shorter wavelengths, applying the same proportional changes to all UV bands leads to an overestimated irradiance change in UV-A and an underestimated one in UV-B-C in SSF2. Without the TSI constraint, SSF1 has only 50% of the TSI change observed by TIM. This large difference in input solar forcing is expected to be a key factor for modeled different temperature responses.

[36] The TOA solar forcing is the input forcing to the climate system. To understand the surface-troposphere temperature responses to solar variations, one needs to examine the profiles of irradiance difference and changes in radiative forcing defined at the tropopause.

[37] First, we examine the vertical profiles of downward spectral solar irradiance difference in Figure 2. From the TOA to the tropopause near ~100 mb, there are large decreases in UV-C and UV-B irradiance differences for both SSF1 and SSF2 due to strong ozone absorption in Hartley bands, small decreases in VIS and UV-A due to Rayleigh scattering and weak Huggins and Chappuis ozone absorption bands, and almost no change in NIR wavelengths, where both scattering and absorption are negligible. The downward SW (UV + VIS + IR) irradiance differences, the direct forcing to the troposphere, are −0.11 and 0.07 W/m^2 for SSF1 and SSF2, respectively.

[38] Now we look at profiles of SW and terrestrial LW irradiance differences in Figure 3. Since the downward SW irradiance difference profiles in Figure 3 are the same as the downward SW irradiance difference profiles in Figure 2, we examine only upward SW, upward and downward LW, and net irradiance variations.

[39] For SSF1, from 2004 to 2007, there is a decrease of 0.06 W/m^2 (Figure 3a, green dashed line) in incident and 0.012 W/m^2 (Figure 3a, green dotted line) in reflected SW

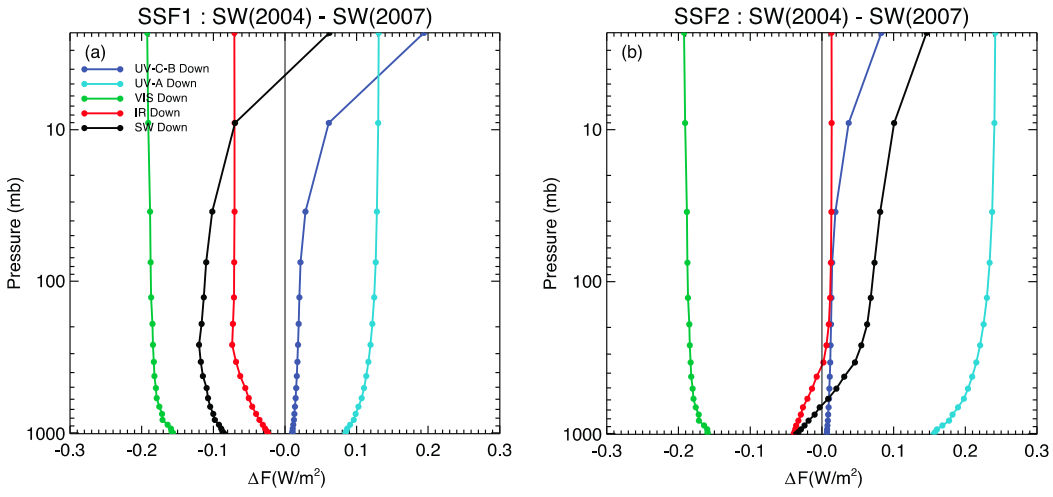

Figure 2. Vertical profiles of solar radiative flux in difference in various spectral bands: (left) SSF1 and (right) SSF2.

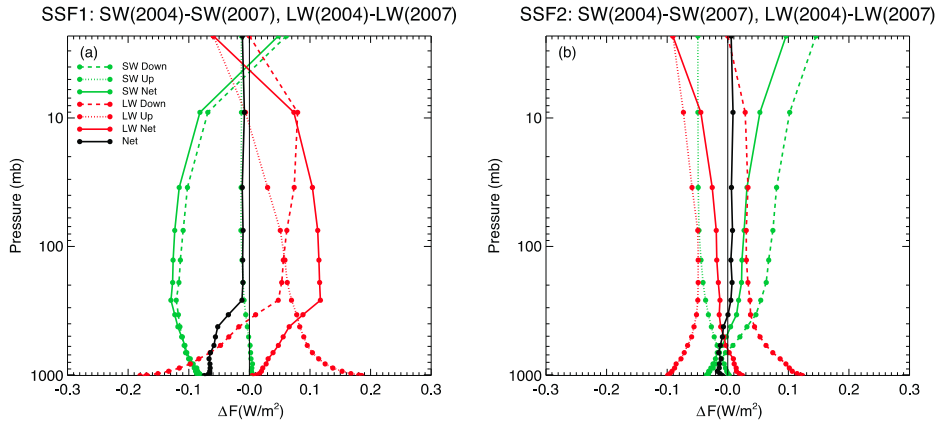

Figure 3. Vertical profiles of SW (green), terrestrial LW (red), and net (black) radiative fluxes: (left) SSF1 and (right) SSF2. Note that we use the convention $F_{\text{down}} > 0$, $F_{\text{up}} < 0$, and $F_{net} = F_{\text{down}} + F_{\text{up}}$.

irradiance difference, respectively. Note that a positive value of 0.012 W/m^2 of upward SW irradiance difference is due to the sign convention in this study. The downward SW irradiance difference depends on altitude due to the wavelength dependence of transmitted spectral solar irradiance as explained earlier. However, the upward SW irradiance difference is almost constant above 250 mb (the top of the high cloud). This is because the most penetrating SW radiation in the troposphere is in UV-A, VIS, and NIR, and reflected irradiances in those wavelengths suffer little attenuation in the stratosphere.

[40] The terrestrial LW irradiance difference profiles are more complicated than those for SW irradiances because LW irradiances depend on the transmission of thermal radiation emitted from other layers [*Liou*, 2002]. For SSF1, the downward LW irradiance difference (Figure 3a, red dashed line) is positive in the stratosphere and upper troposphere, indicating a warmer stratosphere for the active solar year (2004) than for the quiet year (2007). In the troposphere below ~100 mb, the LW irradiance difference decreases toward the surface and becomes negative below 400 mb. This suggests a cooler troposphere for 2004 as compared to 2007. Similarly, the positive upward LW irradiance difference (Figure 3a, red dotted line) in the troposphere indicates a decrease in absolute value from 2004 to 2007 (*or* $|F_{LW}\uparrow(2004)| < |F_{LW}\uparrow(2007)|$) given our upward negative convention. This suggests again a cooler surface and troposphere in 2004 than in 2007. This difference decreases with increasing altitude, suggesting a warming effect in the upper layers that compensates the cooling effect from layers below. In the upper stratosphere near 2 mb, the upward LW irradiance difference becomes negative (or $|F_{LW}\uparrow(2004)| > |F_{LW}\uparrow(2007)|$ in our convention), suggesting that a warming effect in the upper stratosphere dominates the cooling effect from layers below.

[41] Now we examine the profile of net irradiance difference (Figure 3a, black line). We find a small negative net irradiance difference in the upper troposphere and stratosphere. The net radiative forcing at the tropopause near 100 mb is about -0.01 W/m^2. Irradiance profiles and radiative forcing at the tropopause all suggest that the surface-troposphere is cooler in 2004 than in 2007. This is consistent with the RCM's computed equilibrium surface temperature in section 3.3.

[42] For SSF2 in Figure 3b, the SW and LW irradiance differences can be interpreted similarly. At the TOA, the incident downward SW irradiance difference is about 0.14 W/m^2. The negative value of -0.05 W/m^2 in the TOA upward SW irradiance difference (Figure 3a, green dotted line) means an increase in reflected SW irradiance difference of 0.05 W/m^2 from 2004 to 2007. Similar to SSF1, the downward SW irradiance difference depends on altitude due to the wavelength dependence of transmitted solar spectral irradiance, and the upward SW irradiance difference is almost constant above the tropopause near ~100 mb.

[43] Unlike in SSF1, the profile of the downward LW irradiance difference is always positive, and the upward LW irradiance is always negative in SSF2, suggesting a warmer temperature throughout the atmosphere in 2004 than in 2007 (Figure 3b). The net radiative forcing at the tropopause near 100 mb is about 0.01 W/m^2 compared to -0.01 W/m^2 for SSF1. Irradiance profiles and net radiative forcing at the tropopause all suggest that the surface-troposphere is warmer in 2004 than in 2007 for SSF2.

[44] These experiments show that the surface-troposphere temperature is out of phase with solar activity for SSF1 and in phase with solar activity for SSF2. Thus, the difference between the surface temperature response found by C2010 and that implied by the radiative forcing estimate of H2010 is largely, if not entirely, due to the difference in the input solar forcing in the two studies.

3.2. Sensitivity of Radiative Forcing to Ozone Response

[45] In the previous section, we have shown the profiles of the UV, VIS, NIR, SW, LW, and net irradiance differences computed from the RCM for a prescribed ozone amount. In realistic situations, however, stratospheric ozone also responds to changes in solar forcing. The change in stratospheric ozone in turn modulates the spectral solar irradiance reaching the tropopause and consequently influences the surface temperature [*Haigh*, 1994]. To better understand temperature responses to change in solar forcing, one has to consider the ozone response. Since the RCM does not include interactive ozone photochemistry, we have to resort to sensitivity studies.

[46] We run the RCM for the two solar forcing scenarios with uniform changes in total ozone amount. Though the assumption of uniform changes in the ozone profile is not

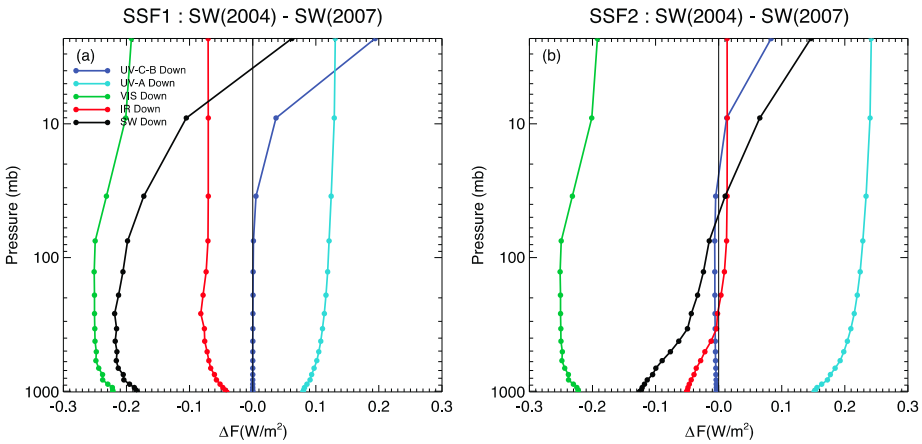

Figure 4. Same as Figure 2 but for a 2% ozone reduction in 2007.

realistic, it does not create large errors in estimating UV-A and VIS irradiance reaching the tropopause and the surface-troposphere temperature responses. This is because both stratospheric ozone and molecular layers are optically thin in these wavelengths ($\tau_{O3} < 1$ and $\tau_{Rayleigh} < 0.1$). The stratospheric transmittance is approximately equal to the product of attenuation due to ozone absorption and transmittance due to molecular scattering. However, changes in the vertical distribution of ozone do affect thermal radiative forcing, which are determined by the lower stratospheric value in our study.

[47] The RCM computed spectral solar irradiance profiles for a 2% change in total ozone (2004 minus 2007) are presented in Figure 4. Since downward irradiances at the TOA are the same as those in fixed ozone experiments in Figure 2, we only examine irradiance differences at the tropopause.

[48] Compared with fixed ozone experiments, the 2% ozone change leads to an even larger decrease of VIS irradiance, a small change in UV-C and UV-B, and no change in UV-A and IR from 2004 to 2007. For SSF1 (Figure 4a), the downward VIS irradiance difference at the tropopause is about -0.25 W/m^2 as compared to -0.18 W/m^2 in the fixed ozone experiment (Figure 2a). This larger decrease in downward VIS irradiance difference for the 2% ozone change experiment can be explained as a result of ozone absorption in the Chappuis bands, as predicted by *Haigh et al*. [2010].

[49] Similar to SSF1, a 2% ozone change in SSF2 leads to a slight change in the UV irradiance difference, no change in the IR irradiance difference, but a significantly large decrease in the VIS and SW irradiance differences at the tropopause near 100 mb (Figure 4b) as compared to the fixed ozone experiment (Figure 2b)

[50] The SW and LW irradiance difference profiles are presented in Figure 5. For SSF1 (Figure 5a), the downward SW irradiance profile (green dashed line) is the same as the black line in the spectral irradiance plot in Figure 4a. At the tropopause near 100 mb, there is a larger net downward SW irradiance difference (-0.18 W/m^2; Figure 5a, green solid line) for the 2% ozone change experiment as compared to that (-0.11 W/m^2; Figure 3a, green solid line) for the fixed ozone experiment. This ozone reduction has the opposite effect on LW. Less ozone will lead to an even cooler stratosphere in 2007 and larger differences in stratospheric temperature and downward LW irradiance between 2004 and 2007. The large decrease in SW irradiance difference (i.e., -0.18 W/m^2 for a 2% ozone reduction as compared to -0.11 W/m^2 for fixed ozone) is largely compensated by a large increase in LW irradiance difference at the tropopause. In fact, the larger positive LW irradiance difference dominates the larger negative downward SW irradiance difference,

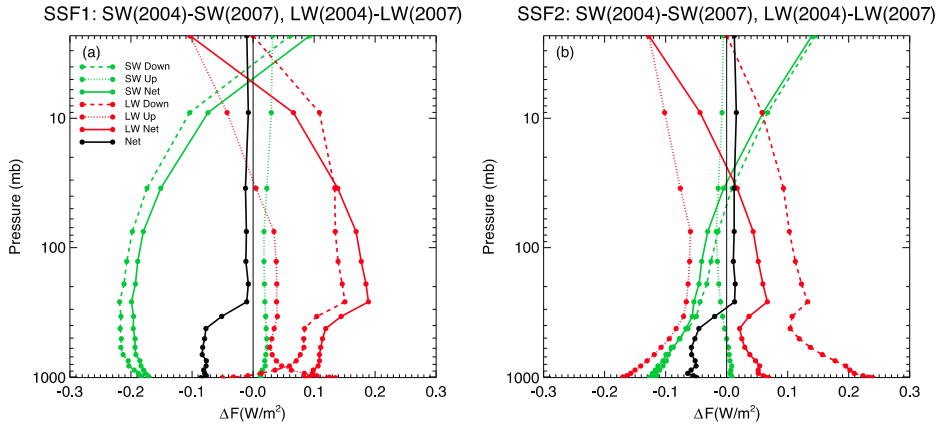

Figure 5. Same as Figure 3 but for a 2% ozone reduction in 2007.

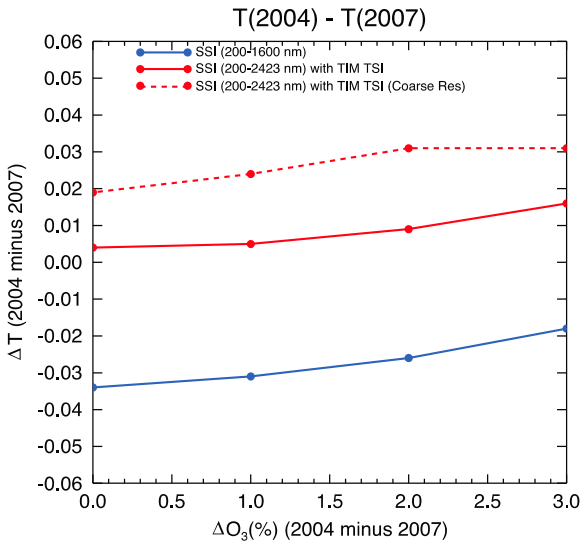

Figure 6. Surface temperature responses to different scenarios of spectral solar forcing with changes in total ozone amount: (blue solid line) SSF1, (red dashed line) SSF2, and (red solid line) SSF3.

resulting in a slightly larger change in net radiative forcing at 200 mb.

[51] We note that the net irradiance forcing differences above 100 mb are similar for both fixed ozone and 2% ozone change scenarios. We have also performed the same experiments for a cloudless atmosphere. We found that the net irradiance forcing differences for a 2% ozone change are consistently larger than those for fixed ozone throughout the stratosphere above 100 mb. Thus, the unnoticeable difference in the net irradiance differences above 100 mb for the two experiments (Figure 5a versus Figure 3a) are likely due to larger errors in small net irradiance differences from two large quantities when clouds are included. Nevertheless, a reduction in ozone amount does lead to a larger surface temperature response, as presented in section 3.3.

[52] For SSF2, a 2% ozone reduction leads to a smaller net downward SW irradiance difference at the tropopause (-0.04 W/m^2; Figure 5b, green solid line) as compared to that for the fixed ozone experiment (0.03 W/m^2; Figure 3b, green solid line). This large decrease in net downward SW irradiance difference is compensated by a large increase in LW irradiance difference, resulting in a slight increase in the net irradiance difference ($\sim$0.01 W/m^2).

[53] The above analysis shows that including the ozone response to the SIM solar forcing alone cannot explain the difference between C2010 and H2010. Rather, it leads to a larger tropopause radiative forcing (2004 minus 2007) and an increase in surface-troposphere temperature response. The following section presents the RCM's surface temperature responses to demonstrate this point.

3.3. Surface Temperature Response

[54] The RCM computes equilibrium temperature responses to various amounts of ozone change for SSF1, SSF2, and SSF3. Surface temperature responses as a function of percent ozone change for the three spectral solar forcing scenarios are presented in Figure 6.

[55] For fixed ozone experiments, the surface temperature response for SSF1 is -0.033 K, out of phase with solar activity, as suggested by H2010. The surface temperature response for SSF2 is 0.02 K, in phase with solar activity, as shown by C2010. The surface temperature response for SSF3 is almost neutral, suggesting the underestimation and the overestimation of temperature responses in H2010 and C2010, respectively.

[56] The temperature response increases with the amount of ozone change for all three forcing experiments. For SSF1, the surface temperature response increases from -0.033 K for the fixed ozone amount and to -0.025 K for the 2% change in total ozone amount (Figure 6, blue solid line). For SSF2, the surface temperature response increases from 0.02 K for the fixed ozone amount and to -0.03 K for the 2% change in total ozone amount (Figure 6, red solid line). For SSF3, the surface temperature response increases from nearly neutral for the fixed ozone amount to about 0.01 K for the 2% change in total ozone amount (Figure 6, red solid line). These results are consistent with the tropopause forcing response to the change in ozone amount presented in section 3.2.

[57] Note that the radiative forcing at the tropopause (and surface temperature change) is (Figures 3 and 5) a small difference of two larger quantities (changes in SW and LW) and indicate (Figure 6) that as ozone goes from 0% to 2%, the LW change (getting more positive) dominates the SW (getting more negative), consistent with the accepted understanding of the factors determining ozone radiative forcing [e.g., *Ramaswamy et al*., 1992].

6. Summary and Discussion

[58] We have performed a detailed study to reconcile apparent differences in radiative forcing and associated surface temperature responses to SIM spectral solar forcing in two earlier studies by *Cahalan et al*. [2010] and *Haigh et al*. [2010]. We found a large difference in input solar forcing variations due to the different ways SIM data were used in the two studies. The RCM was able to produce in-phase and out-of-phase responses similar to those in C2010 and H2010, respectively. We also imitated ozone changes to solar forcing in a sensitivity study and found that the assumption about ozone change alone does not explain the difference between the two studies.

[59] Since the input TOA solar forcing variations for the two studies differ by a factor of 2, we would expect climate models to show different responses when including a radiative-photochemical model such as that used by H2010. Thus, it is imperative that climate modelers take care in the application of SSI data and consider the potential effects on modeled climate response introduced by uncertainties in input solar forcing.

[60] In this paper, we focus on resolving two published apparently contradictory results and consider the direct forcing with a prescribed ozone change in the context of a sensitivity analysis. In the real Earth-atmosphere system, solar-induced stratospheric heat may influence the climate through a "top-down" mechanism [e.g., *Haigh*, 1996; *Kodera and Kuroda*, 2002]; conversely, solar heating of the sea surface and dynamically coupled air-sea interaction may introduce a "bottom-up" mechanism. Recent studies have suggested

that both top-down and bottom-up mechanisms work together to amplify the sea surface temperature, precipitation, and cloud response to relatively small solar forcing [*Rind et al*., 2008; *Meehl et al*., 2009]. Since surface temperature responses to direct forcing are small, and the phase of the response is sensitive to how the SIM-observed SSI is used, an accurate observation of SSI is critical for modeling the Sun-climate connection.

[61] The same way SSI is required for observing the input solar variations, continuous observation of the Earth's reflected and emitted radiation is essential for monitoring the Earth's responses. For climate change studies, observing the reflected solar spectra is more critical than knowing the total reflected energy. The Climate Absolute Radiance and Refractivity Observatory mission will provide accurate observation of spectral radiance reflected and emitted from the Earth [*Wielicki et al*., 2013]. Accurate observation of input solar irradiances from both TSI and SSI and their counterparts from the Earth will be invaluable for climate change studies.

[62] **Acknowledgments.** This research was supported by NASA's Living With a Star program managed by M. Guhathakurta. We also thank A. Arking, J. Lean, W. Ridgway, and D. Rind for helpful discussions.

References

Arking, A. (2005), Effects of bias in solar radiative transfer codes on global climate model simulations, *Geophys. Res. Lett.*, *32*, L20717, doi:10.1029/2005GL023644.

Ball, W. T., Y. C. Unruh, N. A. Krivova, S. Solanki, and J. W. Harder (2011), Solar irradiance variability: A six-year comparison between SORCE observations and the SATIRE model, *Astron. Astrophys.*, *530*, A71, doi:10.1051/0004-6361/201016189.

Cahalan, R. F., G. Wen, J. W. Harder, and P. Pilewskie (2010), Temperature responses to spectral solar variability on decadal time scales, *Geophys. Res. Lett.*, *37*, L07705, doi:10.1029/2009GL041898.

Chou, M.-D., and M. J. Suarez (2002), A solar radiation parameterization for atmospheric studies, *Tech. Rep. Ser. on Global Model. and Data Assim., NASA/TM-1999-104606*, vol. 15, 38 pp.

Chou, M.-D., M. J. Suarez, X.-Z. Liang, and M. M.-H. Yan (2003), A thermal infrared radiation parameterization for atmospheric studies, *Tech. Rep. Ser. on Global Model. and Data Assim., NASA/TM-2001-104606*, vol. 19, 68 pp.

Crommelynck, D., A. Fichot, V. Domingo, and R. Lee III (1996), SOLCON solar constant observations from the ATLAS missions, *Geophys. Res. Lett.*, *23*(17), 2293–2295.

DeLand, M. T., and R. P. Cebula (2008) Creation of a composite solar ultraviolet spectral irradiance data set, *J. Geophys. Res.*, *113*, A11103. doi:10.1029/2008JA013401.

DeLand, M. T., and R. P. Cebula (2012), Solar UV variations during the decline of cycle 23, *J. Atmos. Sol. Terr. Phys.*, *77*, 225–234, doi:10.1016/j.jastp.2012.01.007.

Dickinson, R. E. (1981), Convergence rate and stability of ocean-atmosphere coupling schemes with a zero-dimensional climate model, *J. Atmos. Sci.*, *38*(10), 2112–2120.

Fontenla, J. M., J. Harder, W. Livingston, M. Snow, and T. Woods (2011), High-resolution solar spectral irradiance from extreme ultraviolet to far infrared, *J. Geophys. Res.*, *116*, D20108, doi:10.1029/211JD016032.

Haigh, J. D. (1994), The role of stratospheric ozone in modulating the solar radiative forcing of climate, *Nature*, *370*, 544–546.

Haigh, J. D. (1996), The impact of solar variability on climate, *Science*, *272*, 981–984, doi:10.1126/science.272.5264.981.

Haigh, J. D., A. R. Winning, R. Toumi, and J. W. Harder (2010), An influence of spectral solar variations on radiative forcing of climate, *Nature*, *467*, 696–699, doi:10.1038/nature09426.

Hansen, J., M. Sato, P. Kharecha, and K. von Schuckmann (2011), Earth's energy imbalance and implications, *Atmos. Chem. Phys.*, *11*, 13,421–13,449, doi:10.5194/acp-11-13421-2011.

Harder, J. W., J. M. Fontenla, P. Pilewskie, E. C. Richard, and T. N. Woods (2009), Trends in solar spectral irradiance variability in the visible and infrared, *Geophys. Res. Lett.*, *36*, L07801, doi:10.1029/2008GL036797.

Harwood, R. S., and J. A. Pyle (1975), A two-dimensional mean circulation model for the atmosphere below 80km, *Q. J. R. Meteorol. Soc.*, *101*, 723–747, doi:10.1002/qj.49710143003.

Held, I. M, and B. Soden (2000), Water vapor feedback and global warming, *Annu. Rev. Energy Environ.*, *25*, 441–475.

Ineson, S., A. A. Scaife, J. R. Knight, J. C. Manners, N. J. Dunstone, L. J. Gray, and J. D. Haigh (2011), Solar forcing of winter climate variability in the Northern Hemisphere, *Nat. Geosci.*, *4*, 753–757, doi:10.1038/ngeo1282.

IPCC (2007), *Climate Change 2007: The Physical Science Basis. Contribution of Working Group I to the Fourth Assessment Report of the Intergovernmental Panel on Climate Change*, [S. Solomon, D. Qin, M. Manning, Z. Chen, M. Marquis, K.B. Averyt, M. Tignor, and H. L. Miller (eds.)], 996 pp., Cambridge Univ. Press, Cambridge, U. K. and New York, NY, USA.

Kodera, K., and Y. Kuroda (2002), Dynamical response to the solar cycle: Winter stratopause and lower stratosphere, *J. Geophys. Res.*, *107*(D24), 4749, doi:10.1029/2002JD002224.

Kopp, G., and J. L. Lean (2011), A new, lower value of total solar irradiance: Evidence and climate significance, *Geophys. Res. Lett.*, *38*, L01706, doi:10.1029/2010GL045777.

Kurucz, R. L., and B. Bell (1995), CD-ROM No. 23, Smithsonian Astrophys. Obs., Cambridge, Mass.

Labs, D., and H. Neckel (1968), The radiation of the solar photosphere from 2000 Å to 100 μm, *Z. Astrophys.*, *69*, 1–73.

Lean, J. (2000), Evolution of the Sun's spectral irradiance since the Maunder Minimum, *Geophys. Res. Lett.*, *27*(16), 2425–2428.

Lean, J., and M. T. DeLand (2012), How does Sun's spectrum vary?, *J. Clim.*, *25*(7), 2555–2560, doi:10.1175/JCLI-D-11-00571.1.

Lindzen, R. S., A. Y. Hou, and B. F. Farrell (1982), The role of convective model choice in calculating the climate impact of doubling CO_2, *J. Atmos. Sci.*, *39*, 1189–1205.

Liou, K. N. (2002), *An Introduction to Atmospheric Radiation*, 583 pp., Academic, San Diego, Calif.

Liou, K. N., and S. C. Ou (1983), Theory of equilibrium temperatures in radiative-turbulent atmospheres, *J. Atmos. Sci.*, *40*, 214–229.

Loeb, N. G., B. A. Wielicki, D. R. Doellingm, G. L. Smith, D. F. Keyes, S. Kato, N. Manalo-Smith, and T. Wong (2009), Toward optimal closure of the Earth's top-of-atmosphere radiation budget, *J. Clim.*, *22*, 748–766.

Manabe, S., and R. Wetherald (1967), Thermal equilibrium of the atmosphere with a given distribution of relative humidity, *J. Atmos. Sci.*, *24*(3), 241–259.

Meehl, G. A., J. M. Arblaster, K. Matthes, F. Sassi, and H. van Loon (2009), Amplifying the Pacific climate system response to a small 11 year solar cycle forcing, *Science*, *325*, 1114–1118.

Merkel, A. W., J. W. Harder, D. R. Marsh, A. K. Smith, J. M. Fontenla, and T. N. Woods (2011), The impact of solar spectral irradiance variability on middle atmospheric ozone, *Geophys. Res. Lett.*, *38*, L13802, doi:10.1029/2011GL047561.

Preminger, D., G. Chapman, and A. Cookson (2011), Activity-brightness correlations for the Sun and Sun-like stars, *Astrophys. J. Lett.*, *739*(2), 6, doi:10.1088/2041-8205/739/2/L45.

Ramaswamy, V., M. D. Schwarzkopf, and K. P. Shine (1992), Radiative forcing of climate from halocarbon-induced global stratospheric ozone loss, *Nature*, *355*, 810–812.

Ramaswamy, V., O. Boucher, J. Haigh, D. Hauglustaine, J. Waywood, G. Myhre, T. Nakajima, G. Y. Shi, and S. Solomon (2001), Radiative forcing of climate change, in *Climate Change 2001, Contribution of Working Group I to the Third Assessment Report of the Intergovernmental Panel on Climate Change*, edited by J. T. Houghton et al., pp. 349–416, Cambridge Univ. Press, New York.

Rind, D., J. Lean, J. Lerner, P. Lonergan, and A. Leboissitier (2008), Exploring the stratospheric/tropospheric response to solar forcing, *J. Geophys. Res.*, *113*, D24103, doi:10.1029/2008JD010114.

Rossow, W. B., and R. A. Schiffer (1999), Advances in understanding clouds from ISCCP, *Bull. Am. Meteorol. Soc.*, *80*(11), 2261–2287.

Schlesinger, M. E, W. L. Gates, and Y.-J. Han (1985), The role of the ocean in CO_2-induced climatic warming: Preliminary results from the OSU atmospheric-ocean GCM, in *Coupled Ocean-Atmosphere Models*, edited by J. C. J. Nihoul, 767 pp., Elsevier, New York.

Swartz, W. H., R. S. Stolarski, L. D. Oman, E. L. Fleming, and C. H. Jackman (2012), Middle atmosphere response to different descriptions of the 11-yr solar cycle in spectral irradiance in a chemistry-climate model, *Atmos. Chem. Phys.*, *12*, 5937–5948, doi:10.5194/acp-12-5937-2012.

Thuillier, G., M. Herse, D. Labs, T. Foujols, W. Peetermans, D. Gillotay, P. C. Simon, and H. Mandel (2003), The solar spectral irradiance from 200 to 240 nm as measured by the SOLSPEC spectrometer from ATLAS 1-2-3 and EURECA missions, *Sol. Phys.*, *214*, 1–22.

Wielicki, B. A., et al. (2013), Achieving climate change absolute accuracy in orbit, *Bull. Am. Meteorol. Soc.*, doi:10.1175/BAMS-D-12-00149.1.